Production of hypernuclei in Pb-Pb collisions at $\sqrt{s_{\mathrm{NN}}} = 2.76$ TeV with ALICE at the LHC

Ramona Lea (for the ALICE Collaboration)

Physics Department, University and INFN of Trieste, Via A. Valerio 2, 34127 Trieste, Italy

E-mail: `ramona.lea@cern.ch`

Abstract. Results on (anti-)hypertriton production in Pb–Pb collisions at $\sqrt{s_{\mathrm{NN}}} = 2.76$ TeV, obtained by ALICE at the LHC, are reported. The (anti-)$^3_\Lambda$H signal is extracted exploiting its mesonic decay ($^3_\Lambda$H $\rightarrow$ ^{3}He $+\pi$) , via the topological identification of secondary vertices and the analysis of the invariant mass distributions of (^{3}He, π) pairs. The (^{3}He,π) invariant mass distributions in different transverse momentum and in proper time intervals are shown.
Search for $\Lambda\Lambda$ state (H-Dibaryon) via its decay H-Dibaryon $\rightarrow$ $\Lambda p\pi^-$ is discussed. As no H-Dibaryon signal is observed, an upper limit on its production yield has been determined.

1. Introduction

Ultra-relativistic heavy-ion collisions provide a unique opportunity for understanding the strong interaction: many strange hadrons are produced in the collision and the study of their production yield helps to understand the nature of the space-time evolution and chemical equilibrium of the hadronic fireball. In high-energy heavy-ion collisions hyperon-baryon bound systems, called hypernuclei, can emerge from the hot and dense fireball region of the reaction. Their production yield can be estimated by employing two distinct models: they can be formed via the coalescence of nucleons and hyperons produced in the collision or they can be produced directly in the hadronization process. The study of the production yield of hypernuclei at the LHC energy can help to distinguish between the two models, as the production yield is expected to be different in the two approaches.

Thanks to its unique performance for particle identification, the ALICE detector [1, 2] allows for the measurement of hypernuclei and gives the opportunity to search for predicted states such as H-Dibaryon, a bound state formed by six quarks (*uuddss*) already predicted by Jaffe in 1977 [3] using a bag model calculation. The energy reached at the LHC leads to large production probabilities of such particles, as described for example by thermal models [4, 5, 6].

2. (Anti-) Hypertriton

Hypernuclear physics was born in 1952 when the Polish scientists M. Danysz and J. Pniewski observed the first hypernuclear decay event in a photographic emulsion exposed to cosmic rays at around 26 km above the ground [7]. The hypertriton $^3_\Lambda$H is the lightest known hypernucleus and is formed by a proton, a neutron and a Λ.

The study of the production of ($^3_{\overline{\Lambda}}\overline{\mathrm{H}}$)$^3_\Lambda$H detected via its decay $^3_\Lambda$H $\rightarrow$ ^{3}He $+$ π^- ($^3_{\overline{\Lambda}}\overline{\mathrm{H}} \rightarrow ^3\overline{\mathrm{He}} + \pi^+$) with ALICE will be presented in this section.

2.1. Analysis

For the present study, nearly 20 million of central (0-10%) and nearly 18 million of semi-central (10-50%) events from Pb–Pb collisions at $\sqrt{s_{\mathrm{NN}}} = 2.76$ TeV collected by ALICE during the 2011 run are analysed. The main detector used in the analysis is the Time Projection Chamber (TPC) [8] which has a full azimuthal acceptance for tracks in the pseudo-rapidity region $|\eta| < 0.9$. Both daughter particles of the $^3_\Lambda$H can be identified using the TPC over a wide range of momentum. Once both daughter tracks are identified, it is possible to obtain the hypertriton signal candidates by reconstructing their decay vertices. A set of topological cuts has been implemented in order to reduce the combinatorial background. These cuts include: distance of closest approach (DCA) between the two tracks ($< 0.7\ \sigma$), DCA of the "pion" track from the primary vertex (> 0.4 cm) and cosine of the pointing angle between the line joining the primary and secondary vertex and the the total momentum vector direction (cosine of pointing angle > 0.99). Using the collected statistics it has been possible to obtain a $(^3_\Lambda\overline{\mathrm{H}})\ ^3_\Lambda$H signal, both in central and in semi-central events.

Fig. 1 shows the invariant mass distribution of $[(^3\mathrm{He}+\pi^-)+(^3\overline{\mathrm{He}}+\pi^+)]$ for semi-central events (10-50%) in the transverse momentum range $2 \le p_\mathrm{T} < 10$ GeV/c. Black empty points are the data points while the red histogram is the "like-sign" LS invariant mass spectrum $[(^3\mathrm{He},\pi^+)+(^3\overline{\mathrm{He}},\pi^-)]$. The light curve is the sum of a third-degree polynomial function, used to evaluate the combinatorial background, and a Gaussian function for the signal. The full circles at the bottom of the plot are data after the polynomial background subtraction, and the superimposed black line is the Gaussian fit. A signal with a significance of 3.94 is clearly visible.
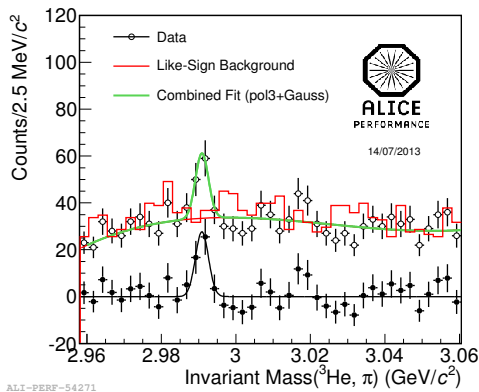
Figure 1. Invariant mass of $[(^3\mathrm{He},\pi^-)+(^3\overline{\mathrm{He}},\pi^+)]$ for semi-central (10-50%) events. See text for more details.
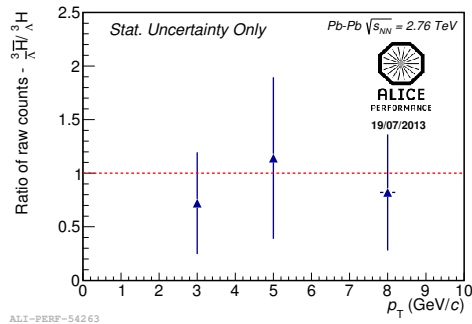

Figure 2. $^3_\Lambda\overline{\mathrm{H}}/^3_\Lambda$H ratio of raw yields versus p_T: this ratio is consistent with unity (reference line) in the whole p_T range. Uncertainties are statistical only.

The collected data allow for the extraction of $^3_\Lambda$H($^3_\Lambda\overline{\mathrm{H}}$) signals in 3 p_T bins: $2 \le p_\mathrm{T} < 4$ GeV/c; $4 \le p_\mathrm{T} < 6$ GeV/c and $6 \le p_\mathrm{T} < 10$ GeV/c. The same procedure to extract the signal described in the previous paragraph has been applied for each p_T bin, and quality checks on the stability of the mean and the width of the signal have been performed. The peak width versus p_T is stable within 2σs, the mean is stable and consistent with the value of $^3_\Lambda$H mass from literature [9].

Fig. 2 shows the $^3_\Lambda\overline{\mathrm{H}}/^3_\Lambda$H ratio of the raw yields versus p_T: this ratio is consistent with the unity (reference line) in the whole considered p_T range.

Using the statistics recorded in 2011 it has also been possible to extract the $(^3_\Lambda\mathrm{H}+^3_\Lambda\overline{\mathrm{H}})$ signal in four ct bins, where ct has been defined as $ct=\frac{MLc}{p}$, M being the nominal value of the $^3_\Lambda$H mass=2.991 GeV/c^2, L the decay length and p the total momentum of the $^3_\Lambda$H candidate.

Fig.3 shows the invariant mass spectrum of the sum of ($^3_\Lambda$H+$^3_\Lambda\overline{\text{H}}$) in two ct bins : $1 \leq ct< 4$ cm (left panel) and $10 \leq ct< 28$ cm (right panel). The empty circle points are the data while full line is the "like-sign" invariant mass spectrum. The light curve is a function which is the sum of a third degree polynomial, used to evaluate the"like-sign" combinatorial background, and a Gaussian for the signal. The full line in the lower part of the plot is the signal extracted after the polynomial background subtraction. A signal is visible in each panel. As soon as the efficiency correction is available the $^3_\Lambda$H lifetime can be determined.
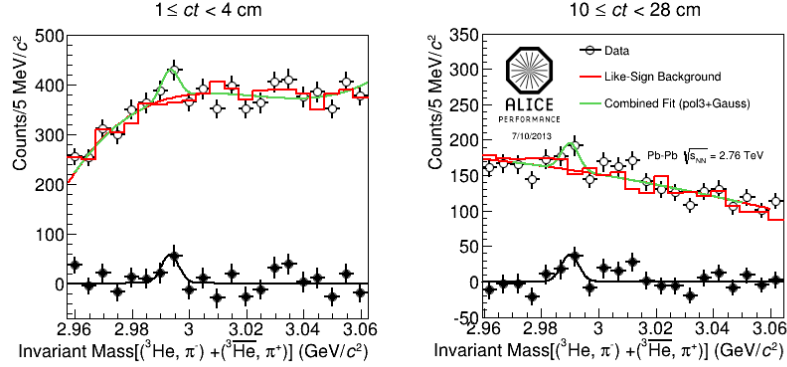
Figure 3. $\left[\left(^3\text{He}, \pi^-\right) + \left(^3\overline{\text{He}}, \pi^+\right)\right]$ invariant mass spectra for 2 *ct* bins. a) [1-4] cm b) [10-28] cm. See text for more details.
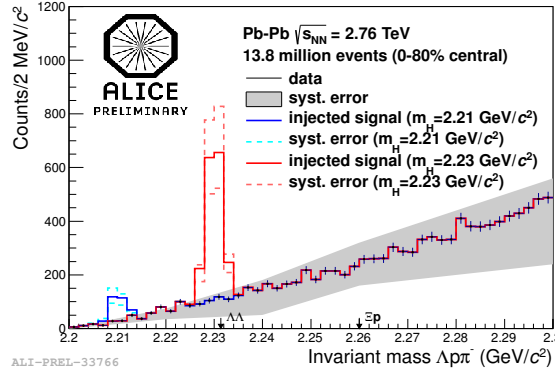
3. H-Dibaryon

Recent lattice calculations [10, 11] suggest that H-Dibaryon should be a bound state, even if those calculations have been performed at an unphysical pion mass ($m_\pi \approx 390$ GeV/c^2). When the results are extrapolated chirally to the pion physical mass [12, 13] the H-Dibaryon is likely to be unbound by 13 ± 14 MeV/c^2 above the $\Lambda\Lambda$ (2.231 GeV/c^2) threshold or even close to the Ξp threshold (2.26 GeV/c^2). A binding energy of around 1 MeV/c^2 is also favored from the observed double-Λ hypernuclei, which gives the current constraints on the $\Lambda\Lambda$ interaction (for a recent review [14] and the references therein). In this analysis decay of the H-Dibaryon into Λpπ has been investigated. Other possible decay channels contain a neutron which is difficult to detect with the ALICE setup. The expected branching ratios depend on the binding energy, as shown in [15]. Since a low binding energy is favored by the current theoretical discussions, the region of mass between 2.2-2.3 GeV/c^2 has been investigated. Considering the H $\rightarrow \Lambda$pπ decay channel, a signal for a bound state would result in a peak in the invariant mass or in a broad structure above the $\Lambda\Lambda$ threshold in case of a resonance. The results shown here for the H-Dibaryon are based on the analysis of about 13.8 million Pb–Pb events in the centrality class of 0-80% taken with the ALICE apparatus in 2010. The reconstructed invariant mass distribution is shown in Fig.4. No evidence of a signal for the H-Dibaryon was found. Fig. 4 also shows the expected signal for the H-Dibaryon for two assumed binding energies: 21 MeV/c^2, which leads to an expected mass of 2.21 GeV/c^2, and 1 MeV/c^2, which corresponds to an expected mass of 2.23 GeV/c^2.

The expected signal was computed estimating the acceptance $\times$ efficiency (from a Monte-Carlo simulation), the production rates as predicted by the thermal-model prediction [16] and the expected branching ratios [17]. In the Monte-Carlo simulation the lifetime of the free Λ hyperon was assumed for the H-Dibaryon. The upper limits for the production yield in the two cases described above, and assuming the thermal model predictions, are reported in Tab. 1. Upper limits have been computed by using a frequentist approach which assumes Poissonian likelihood distributions for background and signal [18, 19].

Particle (Mass /GeV/c^2)	Upper limit of dN/dy (99% CL)
H-Dibaryon (2.23 GeV/c^2)	$\leq 2.0 \times 10^{-4}$
H-Dibaryon (2.21 GeV/c^2)	$\leq 8.4 \times 10^{-4}$

Table 1. Upper limits of dN/dy for the H-Dibaryon at 99% confidence level.

The extracted limits are a factor of 10 lower than the thermal-model predictions used to estimate the expected signal while these successfully describe the yields measured by STAR for the hypertriton [20] within uncertainties. The comparison with other theoretical models can be found in [21].

Figure 4. Invariant mass of $\Lambda + \mathrm{p} + \pi$. The expected signal using thermal-model predictions and the estimated acceptance $\times$ efficiency for two different possible bound states of the H-Dibaryon are also shown.

References
[1] Aamodt K *et al.* (ALICE collaboration) 2006 *J. Phys. G: Nucl. Part. Phys.* **32** 1295
[2] Aamodt K *et al.* (ALICE collaboration) 2008 *JINST* **3** S08002
[3] Jaffe R 1977 *Phys. Rev. Lett.* **38** 195 and erratum ibid 1977 **38** 617
[4] Andronic A *et al.* 2011 *Phys. Lett. B* **697** 203
[5] Cleymans J *et al.* 2011 *Phys. Rev. C* **84** 054916
[6] Petráň M, Letessier J, Petráček J and Rafelski J 2013 CERN-PH-TH/2012-262, arXiv:1303.2098v2 [hep-ph]
[7] Danysz M, Pniewski J 1953 *Phil. Mag. 44* **350** 348
[8] Alme J *et al.* 2010 *Nucl. Instrum. Meth. A* **622** 316-367
[9] Juric M *et al.* 1973 **Nucl. Phys. B 52** 1
[10] Beane S R *et al.* (NPLQCD Collaboration) 2011 *Phys. Rev. Lett.* **106** 162001
[11] Inoue T *et al.* (HAL QCD Collaboration) 2011 *Phys. Rev. Lett.* **106** 162002
[12] Shanahan P E, Thomas A W, Young R D, 2011 *Phys. Rev. Lett.* **107** 092004
[13] Heidenbauer J, Meiner U G 2011 *Phys. Lett. B* **706** 100
[14] Botta E, Bressani T, Garbarino G 2012 *Eur. Phys. J. A* **48** 41
[15] Schaffner-Bielich J, Mattiello R, Sorge H 2000 *Phys. Rev. Lett.* **84** 4305
[16] Andronic A, private communication
[17] Schaffner-Bielich J private communication
[18] Rolke W, Lopez A 2001 *Nucl. Inst. Meth. A* **458** 745
[19] Rolke W, Lopez A, Conrad J and James F 2005 *Nucl. Instr. Meth. A* **551** 493
[20] Abelev B I *et al.* (STAR Collaboration) 2010 *Science* **328** 58
[21] Dönigus B (for the ALICE Collaboration) these proceedings